IEEE Access
Multidisciplinary ⋮ Rapid Review ⋮ Open Access Journal

Received 4 September 2023, accepted 17 September 2023, date of publication 22 September 2023,
date of current version 28 September 2023.

Digital Object Identifier 10.1109/ACCESS.2023.3317999

RESEARCH ARTICLE

Analysis and Improvement of Bandwidth and Gain of Millimeter-Wave Microstrip Franklin Antenna With Proximity-Coupled Feed

AHMAD FIRDAUSI[1], (Student Member, IEEE), GAMANTYO HENDRANTORO[1], (Senior Member, IEEE), EKO SETIJADI[1], (Member, IEEE), AND MUDRIK ALAYDRUS[2], (Senior Member, IEEE)

[1]Department of Electrical Engineering, Institut Teknologi Sepuluh Nopember, Surabaya 60111, Indonesia
[2]Department of Electrical Engineering, Universitas Mercu Buana, Jakarta 11650, Indonesia

Corresponding author: Gamantyo Hendrantoro (gamantyo@ee.its.ac.id)

This work is made possible by a graduate scholarship funding awarded to Ahmad Firdausi by the Center for Higher Education Funding (BPPT) and the Educational Fund Management Institution (LPDP) of the Indonesian Ministry of Finance through the Beasiswa Pendidikan Indonesia Program No. 202101121577.

ABSTRACT In this paper, analytical equations drawn from previous literature on Franklin antenna designs are combined to provide a single solution with an objective of increasing the bandwidth and impedance gain. We adopt the method of a collinear planar antenna as realized in the Franklin antenna, which can reduce the dimensions of the antenna. The main advantage of using the Franklin antenna is that it has a high gain due to the structural characteristics of an array, but it results in a narrow bandwidth. Therefore we combine the Franklin array technique with the proximity couple feeding that can eliminate radiation scattering and can provide large bandwidth. The combined application of the two techniques aims to increase the impedance bandwidth and gain, jointly verified through simulation and measurement with similar results. A stringent full-wave solution is used to evaluate the suggested model, and an experimental antenna prototype is developed. The results for bandwidth and gain from the equations are found to be very similar to those from the simulation and measurement results. Specifically, from the simulation the largest bandwidth is 8.39 GHz with a frequency range of 26.96 - 35.35 GHz and a gain of 11.55 dBi at the frequency of 28 GHz, while the largest measured bandwidth is 9.34 GHz spanning a frequency range of 21.96 - 31.06 GHz. The difference between the analytical model proposed by simulation and measurement is less than 5%. This also shows that the microstrip Franklin antenna with proximity coupled feed (MF-PCF) is a strong candidate for 5G applications.

INDEX TERMS Franklin antenna, proximity coupling feed, wide bandwidth, high gain, millimeter-wave, 5G, microstrip antenna.

I. INTRODUCTION

The development of 5G technologies that support the demand for enhanced mobile broadband (eMBB), ultra-reliable and low latency communication (uRLLC) in around 2017-2024 is estimated to cover low-band (<1GHz), mid-band (1-6GHz), and high-band (mmWave). The mmWave frequency is predicted to be used in fixed wireless access (FWA), backhauling, and network slicing services which acquire 12 dBi of gain [1], [2], [3]. Customer premise equipment (CPE) availability is highly considered and responded to by smartphone vendors by releasing FWA devices [4]. The Federal Communication Commission (FCC) proposes 5G wireless broadband frequencies starting from 3.5-6 GHz [5], 27-40GHz, and 64-71 GHz bands [6].

One of the technologies that have wireless applications nowadays is 5G mobile communications. 5G wireless mobile communications that employ millimeter-wave offers high-speed wireless information transfer [7].

The use of millimeter-wave frequency impacts a decrease in mobile phone antenna dimensions. The conventional antennas were replaced with a microstrip antenna structure

The associate editor coordinating the review of this manuscript and approving it for publication was Tutku Karacolak.

[8]. Microstrip antennas (MA) are supposed to be highly recommended candidates due to their simplicity, high reliability, and compact geometry [9], [10]. Microstrip Antenna (MA) is a widespread type that is very easy to build. On the other hand, it produces narrow bandwidth and low gain, representing the weakness of MA conventional [11], [12]. An array technique is needed [13]. The arrangement of antennas in an array can increase the gain and directivity of an antenna [14] so that the direction of the antenna beam becomes more directional.

Several previous studies have used the parasitic patch method to increase bandwidth and gain [15], [16], [17], [18], [19]. Two methods underlie the parasitic patch method: the coplanar technique and the stacked technique. In the coplanar technique, different patches are joined on top of the substrate, and one patch between different radiator patches is given an excitation called the main patch. In contrast, in the stacked technique, one patch is used on top of another patch by replacing the dielectric layer allowing two or more patches to be distributed to each other aperture area [20]. The weakness of the parasitic patch method is that the antenna design occupies more space which will cause big problems when designing a compact-size broadband antenna, and the results of using the parasitic patch method will produce multiband frequencies, so it is not suitable for being applied to research that focuses on one frequency range [21].

Another study reported a gain enhancement technique using the electromagnetic bandgap (EBG) method, which was combined with the air layer on the microstrip patch antenna using a coaxial probe feeder the design resulted in a gain of 6.5 dBi [22], [23], [24].

Some researchers tried to combine the proximity-coupled method with other antenna methods to increase bandwidth, the combination of the proximity-coupled method with tuning stubs to increase the bandwidth by about 8.4% [25], a dipole antenna-based proximity couple using coaxial feeding [26], a 6 × 5 proximity coupled planar array has been made for 5G applications with a 9.8% bandwidth and 21 dBi gain [27], novel proximity-coupled-fed patch antenna with increased impedance bandwidth [28]. The advantage of the proximity coupled method is that it has a channel that can eliminate radiation spread and provide very high bandwidth due to the increase in the overall thickness of the microstrip antenna [29].

Previous research has combined the proximity couple method with a patch array microstrip antenna. The result of this combination is a significant increase in the performance of a broadband microstrip antenna without increasing the complexity of the antenna design, size, and cost [30].

Research on the dipole array antenna, which is the basis of the Franklin antenna, was carried out to see the array performance using dipole element multiplication and array factor [31]. Franklin originated the concept in 1924 [32]. First, he developed a collinear array (CoA) from a long wire with λ/4 U-shaped sections to produce a phase shift in order to preserve in-phase feeding of straight λ/2 portions of the wire (Figure 1). Nishimura first introduced the microstrip

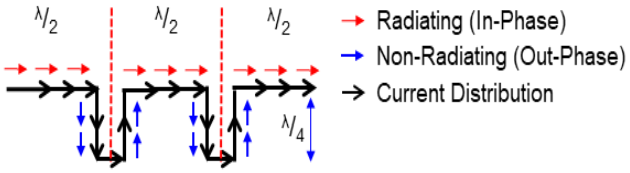

FIGURE 1. The basic structure of the Franklin antenna.

line antenna that applies the Franklin method. In principle, Nishimura utilizes a curved path as a non-radiating path, which results in an out-phase reflection [33].

By utilizing non-radiating quarter-wave stubs, Franklin changed the initial out-phase current distribution into an in-phase one on the collinear segments (solid red arrows in Figure 1), producing a single primary radiation beam. The high gain resulting from the antenna array structure is a fundamental advantage of this arrangement, but the simplicity of the single feeding point is preserved. The proximity-coupled feeding approach, which is one of the non-contact feeding methods [34], offers greater bandwidth (as much as 13%) than other feeding strategies that require direct contact between the feed line and the radiating patch, such as the probe-fed and edge-fed systems.

The conventional microstrip Franklin (MF) is based on CoA principle, composed of a series of radiating elements provided with an in-phase feeding that offers high-gain performance [35], [36], [37]. Several papers reported modifications of the Franklin antenna arrays to achieve high gain [38], [39], [40]. However, CoA has its critical limits, namely narrow-band and single-frequency operation.

A modified microstrip Franklin array (MFA) is a compact 2-D array where the conventional CoA principle has intentionally deviated to realize multiple resonances at the millimeter-wave spectrum. Such a technique has been shown to produce a gain of 13.5 dBi at 29 GHz even with a very simple geometry [41], whereas a multiband MFA produces 1.16 GHz bandwidth spanning 20.34-21.5 GHz [42] and a modified MF yields a wide bandwidth of 9.4 GHz covering 23.6-33 GHz [10].

The proximity coupled feeding (PCF) is recommended for use in MFA due to its bandwidth enhancement and matching features proven. For instance, a compact mmWave array antenna with PCF yields a gain of 14.8 dBi-15.6 dBi and bandwidth enhancement of 6.98% [30]. A typical increase in gain due to PCF ranges from 16% [43]. While [29] shows the application of PCF on an array MA that successfully yields a measured bandwidth of 11.5 GHz, proximity couple method can increase bandwidth by 13% according to [44].

With the above considerations, this paper adopts and modifies the concept of the collinear planar antenna arrangement exhibited by the Franklin antenna to reduce its size. The main advantage of using this is the high gain characteristic of an array arrangement, although the Franklin structure results in a narrow bandwidth. We combine the Franklin technique

TABLE 1. Specification of the substrate used.

Specification	Value
Dielectric constants ($\mathcal{E}_r$)	2.2
Dielectric loss tangent (tan δ)	0.0013
Thickness (h)	1.57
Substrate Material	Rogers 5880

with the PCF to compensate for the narrow-band nature to eliminate radiation scattering and provide wider bandwidth. This is due to the increased overall thickness of the microstrip antenna and the easier matching process. The increases in gain and bandwidth are demonstrated by simulation and measurement.

The following are our contributions:

1) Previously, Franklin antenna modifications focused only on one parameter, namely gain. We develop a basic design of microstrip Franklin antenna that incorporates the proximity coupled feed (MF-PCF) to achieve high gain and bandwidth at the same time. The superior performance of our design is demonstrated by simulation and measurement. The novelty can be described by Fig. 2 in the paper, in which part (a) represents modified conventional Franklin that has been proposed before, while part (b) shows the new proposed design in the form of MF-PCF structure. The superior performance of the new design compared to the previous designs is given in Table 6 in the paper.
2) Since previous studies have not yet provided a complete set of expressions for geometry of the structure of Franklin antenna, in this paper we give the necessary expressions unified from various literatures, which is given by equations (1)-(13). We also provide a procedure to find the geometric structure of the MF-PCF using the expressions, as described in Section II (Design Method).

This paper also draws from previous Franklin antenna design papers [42], [43], [44], [45], [46], which individually provide the mathematical formulation of different parameters of the Franklin, which are combined herein to obtain the desired MF-PCF antenna design.

The remaining sections of this paper are structured as follows: In Section II, the mathematical equations from the previous literature and the antenna design are reviewed. In Section III, the antenna design is analyzed parametrically, whereas in Section IV the fabrication details of the antenna prototype and its performance assessment are shown. Finally in Section V conclusions are given.

II. DESIGN METHOD

The antenna consists of two substrate layers with six Franklin elements arranged linearly with a space of 0.5 λo from the top layer, where λo denotes the free space wavelength. In this modified design, the patch is removed because the transmission line has taken over its role in the lower layer, but later on in this section an expression related to the patch is still needed because the results of the patch width (W_p) are used to find the slot length of Franklin element (L_s) and the width of the antenna ground (W_g). The substrate is a dielectric material that has a constant dielectric value (ε_r), thickness (h), and loss tangent (tan δ). These three parameters affect the designed antenna performance, such as the working frequency, bandwidth, gain, and efficiency. Table 1 provides information related to the substrate used in the research.

We use a resonant frequency of 28 GHz. To calculate the dimensions of the designed antenna, we use reference calculations from [45]. To determine the wavelength λ_d in the substrate, we apply:

$$\lambda_d = \frac{c}{f_r\sqrt{\epsilon r}} \tag{1}$$

where c represents the speed of light 3.00×10^8 m/s, ε_r denotes the relative dielectric permittivity of the substrate, and f_r represents the resonant frequency. In the proposed antenna design, the element uses a stub consisting of two lengths of 0.25 $\lambda_0(L_{st})$ and stub width $W_{st} = W_s + 2C_{\text{arm}}$.

We use a λ/4 line impedance transformer, one of the Chebyshev impedance transformer methods to calculate the slot width [46], having an impedance of:

$$Z_t = \sqrt{Z_l Z_0} \tag{2}$$

where Z_0 denotes the characteristic impedance of the transmission line and Z_l denotes the un-matched load impedance. In our case, Z_l is $2 \times Z_0 = 2 \times 50 = 100\ \Omega$.

Next, we apply the expression for total radiation conductance to calculate the size of the slot and C_{arm} on the Franklin element stub [47],

$$G = \frac{1}{45}\left[\frac{W}{\lambda o}\right]^2 \tag{3}$$

$$w = \lambda_0\sqrt{\frac{45}{Z_t}} \tag{4}$$

$$W_s = \frac{w}{nF} \tag{5}$$

$$C_{\text{arm}} = \frac{Ws}{2} \tag{6}$$

where w represents the total width of the slot on the Franklin element stub, using six elements the resulting total slot width is 8.5 mm. The size of each the slot width (W_s) which can be obtained using (5). Which in turn is used to calculate the slot length (L_s) and the total length (L_{tf}) contained in the Franklin antenna elements,

$$L_s = 2L_{st} + W_p \tag{7}$$

$$L_{tf} = L_s + 2C_{\text{arm}} \tag{8}$$

The total length L_{fe} of all Franklin elements, a total of six in this study, can be calculated using

$$L_{fe} = n_F L_p + 2n_F C_{\text{arm}} + n_F W_s \tag{9}$$

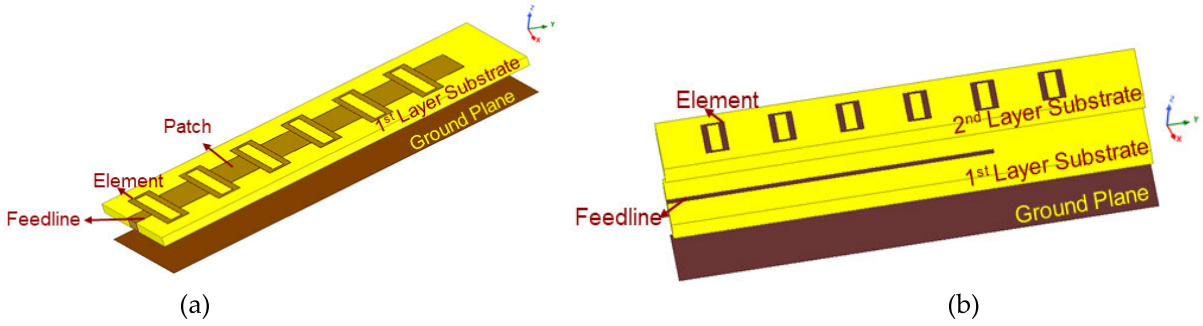

FIGURE 2. (a) modified conventional Franklin antenna structure, (b) MF-PCF modified Franklin antenna structure.

In calculating L_p we apply [48],

$$L_p = \lambda_o/2 \tag{10}$$

where the total number of Franklin elements used are denoted by n_F, whereas L_p denotes the inter-element spacing. Furthermore, to calculate the length L_g and the width W_g of the ground from the antenna we use

$$L_g = L_{fe} + n_F h \tag{11}$$

$$W_g = W_p + 2(L_{st} + C_{arm}) + n_F h \tag{12}$$

In the original Franklin antenna design, the patch line width is denoted by W_p. Although our design, to be described later, does not use such a patch line, the calculation of the patch line width is needed to obtain other parameters. Herein it is found for a patch line impedance of $\frac{50}{\sqrt{2}}$ Ω by applying [49],

$$W_p = \frac{2h}{\pi}[B - 1 - ln(2B - 1) + \frac{\varepsilon r - 1}{2\varepsilon r}] \times [ln(B - 1) + 0.39 - \frac{0.61}{\varepsilon r}]$$

$$B = \frac{60\pi^2}{Zo\sqrt{\varepsilon r}} \tag{13}$$

To calculate the width W_f and the length L_f of the 50 Ω proximity transmission line, we use [50],

$$W_f < 0.25\lambda_d \tag{14}$$

$$L_f = 0.5\left(L_g - L_p\right) + (R_p L_p) \tag{15}$$

where:

$$R_p = X_1 h_{1\lambda d}{}^3 + X_1 h_{1\lambda d}{}^2 + X_1 h_{1\lambda d} + X_4 = 4.34$$

$$X_1 = 73.75\varepsilon_r - 834.9\varepsilon_r + 3129 = 1454.47$$

$$X_2 = -149.9 - 257.1e^{-0.1708\varepsilon_r{}^2} = -262.38$$

$$X_3 = 0.2772\varepsilon_r{}^2 - 2.489\varepsilon_r + 8.502 = 4.367$$

$$X_4 = 0.89$$

$$h_{1\lambda_d} = \frac{h_1}{\lambda_d} = 0.217 \text{ mm}$$

The parameters of the Franklin antenna are obtained through the following steps:

TABLE 2. Resonator parameters of the equivalent circuit.

	Cp	*Lp*	*Rp*
1st Resonator	2.27 pF	23.57 pH	40 Ω
2nd Resonator	42.7 pF	1 pH	10 Ω
3rd Resonator	1.8 pF	18.1 pH	30 Ω
4th Resonator	27 pF	1.1 pH	15 Ω
5th Resonator	23.6 pF	1 pH	20 Ω
6th Resonator	20.8 pF	1 pH	25 Ω

(i) Assign the resonant frequency f_r, i.e., by calculating the free-space wavelength λ_o.
(ii) Next, calculate wavelength of the material λ_d using (1)
(iii) Width of the slot W_s and the width of the Franklin element C_{arm} are calculated using (3)-(6).
(iv) Use 0.25 λ_0 for stub length (L_{st}), the Franklin element spacing (L_p), width (W_g), and length (L_g) of the ground plane (10)-(12).

A. MF-PCF ANTENNA STRUCTURE

HFSS is used to carry out modelling, simulation, analysis, and numerical evaluation of the antenna with geometry obtained by applying equations (1)-(15). The proposed modified Franklin structure is based on a collinear array structure. We calculate the stub, slot, C_{arm}, and Franklin element spacing. See Table 3 for the parameter values of the antenna obtained from the equations. Figure 3 shows the MF-PCF antenna structure, including (a) the 2D sketch of the MF-PCF, (b) the 3D sketch, (c) the equivalent circuit model, and (d) a comparison in reflection factor of the equivalent circuit and simulation based on the mathematical equations.

The structural design of the MF-PCF antenna has two substrate layers. The first substrate layer consists of a ground plane on the lower side and a feedline on the upper side of the layer, while the second on the upper side consists of Franklin elements which in this study are six in total. The two substrates are stacked and referred to herein as the first and the second substrate layers. From a circuit

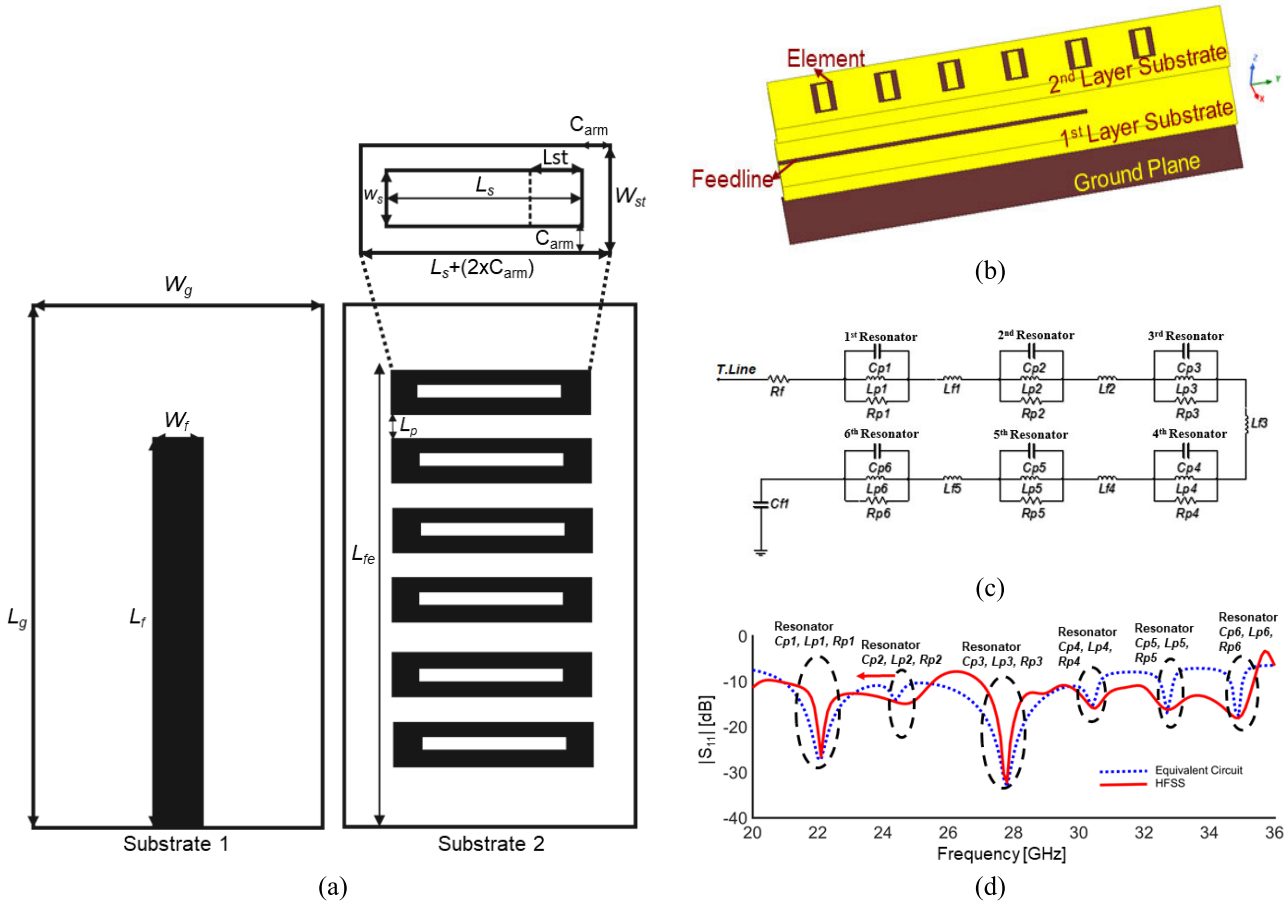

FIGURE 3. (a) 2D sketch of the MF-PCF structure, (b) 3D sketch of the MF-PCF structure, (c) the equivalent circuit model, (d) comparison of reflection factor of the equivalent circuit and simulation based on the mathematical equations.

perspective, the MF-PCF can be modelled as an *RLC* parallel resonator in series with an equivalent circuit of the feed section. In Figure 3(c), six series of R, L, and C are used as resonators to produce a curve similar to the results of applying the equations. The values of L and C determine the resonant frequency. We use the equation below [51], [52].

$$f_r = \frac{1}{2\pi\sqrt{LC}} \tag{16}$$

Figure 3(d) illustrates the comparison of the equivalent circuit versus the results from the HFSS simulation of the calculated model, revealing a high degree of similarity. The patch RLC circuit is entirely defined by the resonant frequency [53], and the design carried out in this study is based on previous mathematical calculations to produce a Franklin antenna structure. T.Line in Figure 3(c) represents the 50 Ω transmission line.

B. DIRECT LINE vs PCF

The simulation results of return loss from the six-element Franklin based on the equations are shown in Figure 4. We can see the antenna simulation results for the direct line-fed Franklin and the MF-PCF. Taking −10 dB return loss as a reference for bandwidth calculation, the direct-line Franklin (dotted line) works best at 28.8 GHz with a total bandwidth of around 2.77 GHz, while the MF-PCF (solid line) shows that the best frequency is 27.8 GHz with a total bandwidth of around 8.54 GHz. It can be seen that there is a very significant increase in bandwidth from the use of proximity-coupled feeding compared to the use of feeding direct line. That is, properly adding the proximity-coupled method can result in a significant increase in bandwidth.

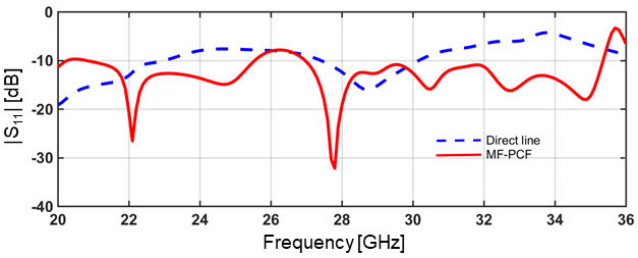

FIGURE 4. Simulation of Franklin Direct Line and MF-PCF.

As seen in Figure 5 (a) and (b), at 28 GHz the gain of direct line-fed antenna is 9.59 dBi, whereas for the MF-PCF it is

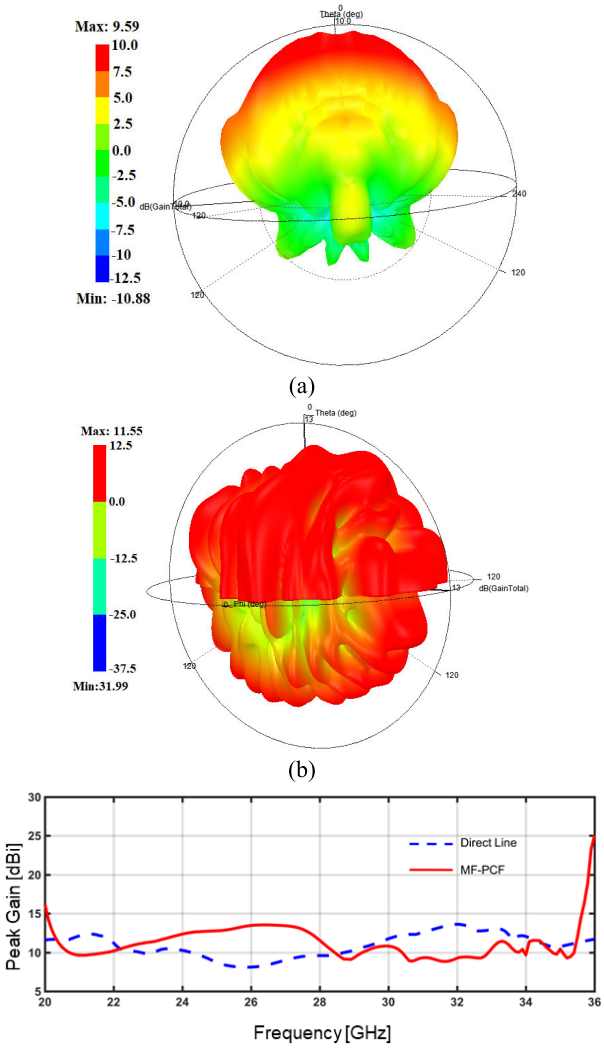

FIGURE 5. (a) Gain 3D for Direct line (b) Gain 3D for MF-PCF (c) Gain Direct line vs MF-PCF.

11.55 dBi. Figure 5 (c) shows the superimposed curves of direct line-fed and MF-PCF maximum gain over the spectrum of interest. Figure 4 also shows that not only does the addition of the proximity-coupled feeding technique increase the bandwidth, but it also increase gain, in agreement with the previous research [30]. Table 4 shows simulation results for the two excitation methods.

Figure 6 shows the formula-based radiation patterns at $\varphi =$ 0° and 90° with direct-line feed and PCF at 28 GHz. It shows that there are more than one major lobe generated by the radiation pattern. The emission of multiple major lobes is probably affected by the element spacing L_P.

III. PARAMETRIC ANALYSIS OF MF-PCF

A. NUMBER OF ELEMENTS

Figure 7(a) shows the return loss of the MF-PCF antenna. It can be seen that the largest bandwidth is obtained with a six-element antenna design, namely a total bandwidth of

TABLE 3. Antenna dimensions obtained from mathematical equations.

Parameters	Size (mm)
Transmission line width (W_f)	1.8
Transmission line length (L_f)	39.5
Patch width (W_p)	7.9
Franklin array element spacing (L_p)	5.35
Width (C_{arm})	0.7
Franklin element stub width (W_{st})	2.8
Franklin element stub length (L_{st})	2.7
Slot width (W_s)	1.4
Slot length (L_s)	13.3
Franklin total length (L_{tf})	14.7
6 element Franklin length (L_{fe})	48.9
Ground length (Lg)	58.32
Ground width (W_g)	24.12

TABLE 4. Simulation results using two excitation methods.

Parameters	MF-PCF	Direct Line Feeding
Resonant frequency	27.8, 22.1 GHz	28.7 GHz
Gain	11.55 dB	9.59 dB
Lowest return loss	-32.2 dB	-16.0 dB
Bandwidth	8.39 GHz (26.96–35.35 GHz) 4.75 GHz (20.80-25.55 GHz)	2.77 GHz (27.40-30.17GHz)

13.14 GHz. With the best resonant frequency that is closest to the calculation is 27.8 GHz. Furthermore, Figure 7(b) demonstrates that the highest gain, which is 11.55 dBi, is certainly obtained with the largest number of elements, i.e., six of them. Hence, it can be concluded that the number of elements in the MF-PCF antenna affects both bandwidth and gain.

B. ELEMENT SPACING

In Figure 8(a) it can be seen that changing the element spacing L_P can result in a reduced HPBW value when the element spacing gets smaller. The gain of each element does not change even if the spacing changes. As a conclusion, the HPBW increases according to the number and spacing of the elements, whereas the gain value increases according to the number of elements used. Figure 8(b) shows the E-plane HPBW for center frequencies of 23, 25, 27, 28, 29, 31, 33 and 35 GHz. It can be seen that the highest HPBW occurs at 25 GHz and the lowest at 35 GHz.

Fig. 9(a) reports optimization result for element spacing L_P. It is apparent that the element spacing affects the variation of return loss against frequency in the band of interest. The previous spacing of 5.35 mm produces return loss of

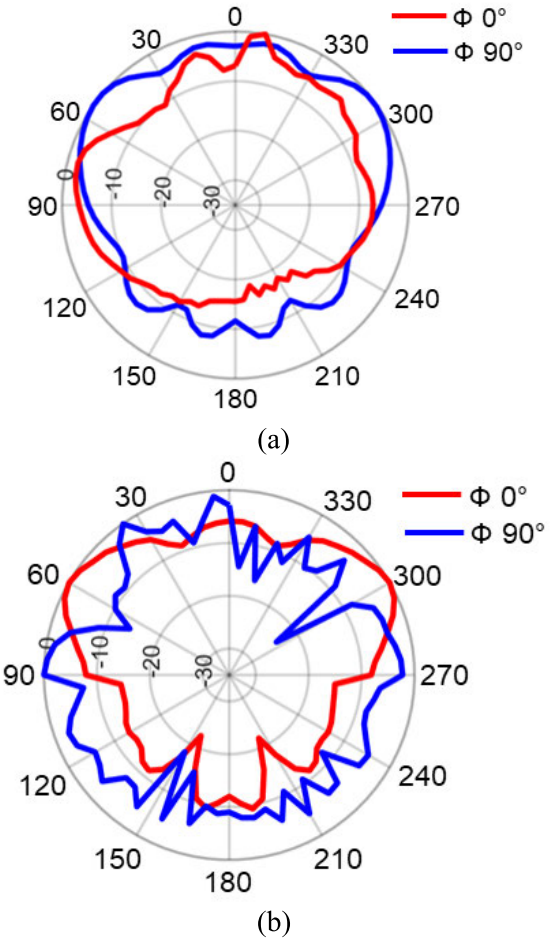

FIGURE 6. Radiation pattern at Φ =0° and Φ =90° at 28 GHz (a) Direct line (b) MF-PCF.

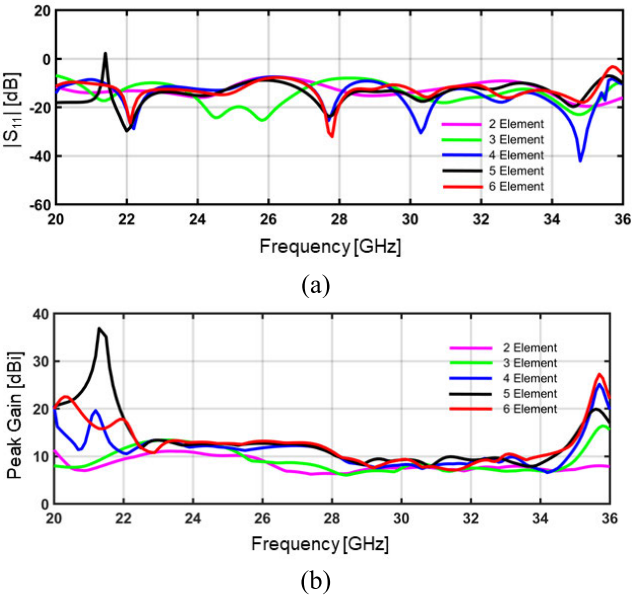

FIGURE 7. MF-PCF performance with different number of elements in (a) return loss and (b) gain.

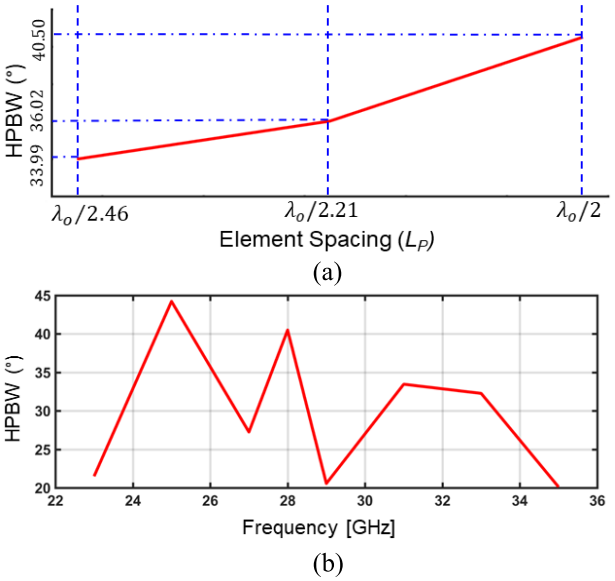

FIGURE 8. Variation of E-plane HPBW with respect to (a) Element Spacing at Frequency 28 GHz and (b) Frequency at element spacing $\lambda_o/2$.

−32.2 dB at 27.8 GHz. Changing the element spacing from $\lambda_o/2$ to $\lambda_o/2.21$ and finally to $\lambda_o/2.46$ results increase in the return loss, the least of which is −29.6 dB occurring at 22.1 GHz.

In Figure 9(b), the pattern is observed on the y-z plane when the element is positioned along the y axis. With half-wavelength spacing, a radiation pattern is obtained with two main lobes in the ±60° direction and a smaller lobe in the 0° direction with a magnitude of around 5 dB below the peak. When the spacing is reduced, the two major lobes shift closer to one another while the smaller lobe at 0° fades. The appearance of the two major lobes is beneficial to capture as many scattered waves coming from various directions as possible, as well as to compensate for scan-loss due to reduction in effective aperture at large angles.

C. NUMBER OF ELEMENTS PASSED BY FEED LINE

Figure 10 demonstrates surface current of 1-element and 6-element antenna at 28 GHz. A high current density is observed in the antenna feedline and each stub element through which the feedline passes. However, one stub element not traversed by the feedline has a low value for current density; this implies that the current density will increase if the feedline crosses the stub element. three major lobes are generated in this case to produce a multi-lobe, which can be obtained by setting the distance from L_P. This antenna is designed to be operated in the frequency band of interest. and can be integrated into cellular 5G. The antenna with the proposed dimensions is the strongest candidate for the technology, as it gives high bandwidth and gain.

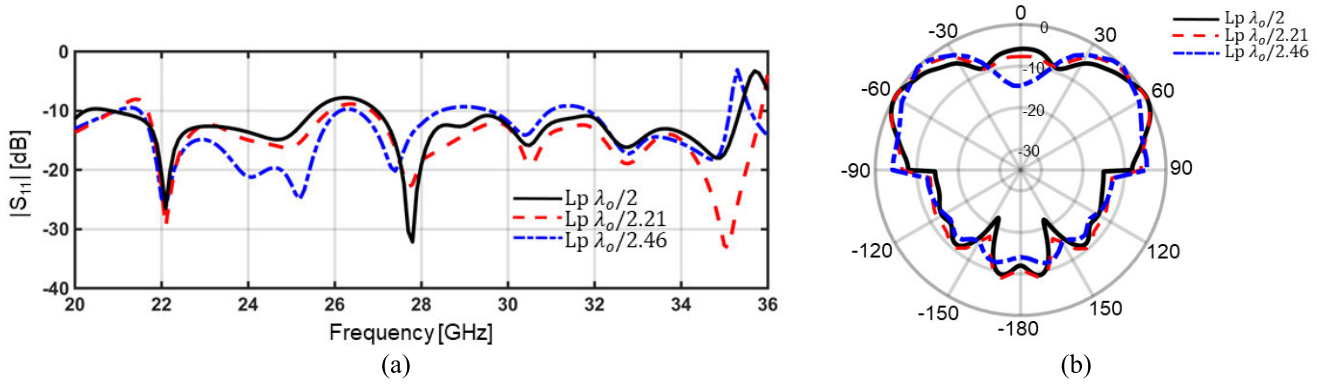

FIGURE 9. Effects of variation in element spacing L_P on (a) return loss and (b) radiation pattern at 28 GHz.

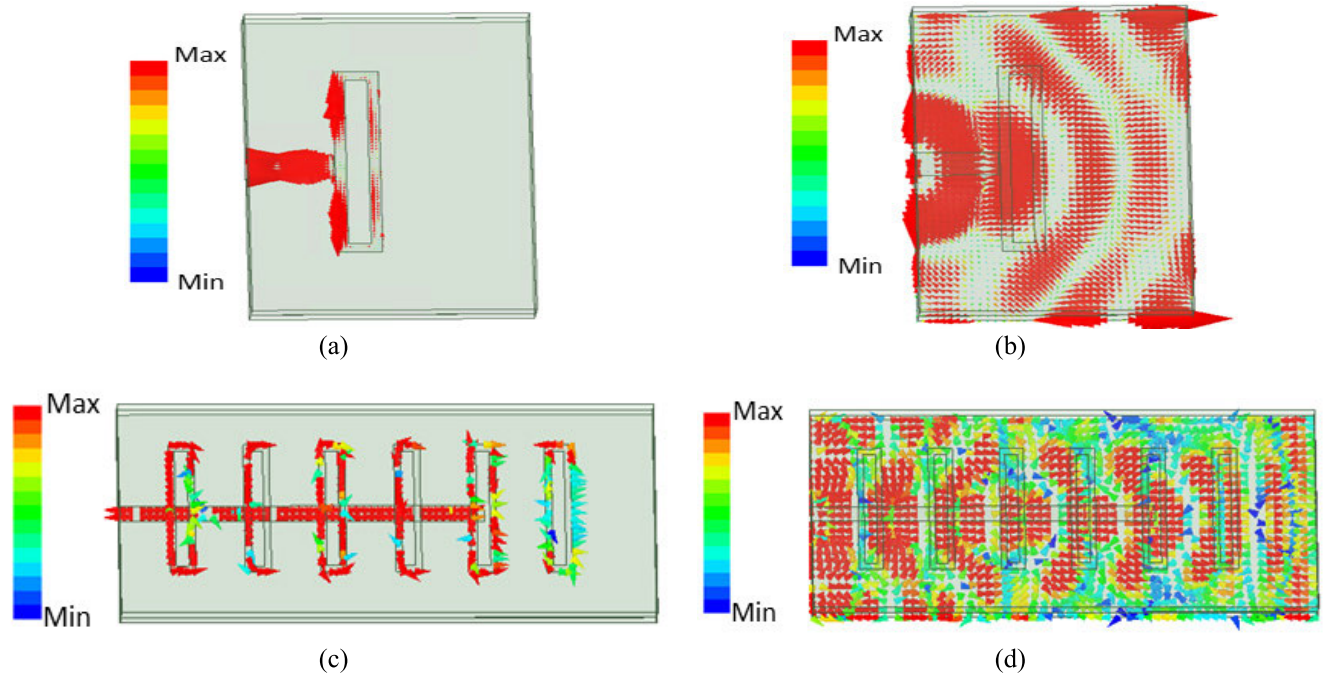

FIGURE 10. Surface current distribution on a single element: (a) the element and feedline layers, (b) the element, feedline and ground layers superimposed and on a six-element Franklin (c) the elements and feedline layers, (d) the elements, feedline and ground layers superimposed.

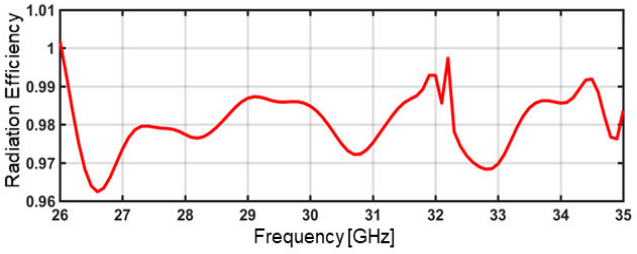

FIGURE 11. Radiation efficiency vs frequency of proposed antenna.

D. ANTENNA MATERIALS

As shown in Figure 11, the radiation efficiency of the proposed antenna is 0.9774 at 28 GHz. The radiation efficiency, i.e., the ratio of the antenna radiated power to the input port supplied power, taking into account the material dielectric loss from copper and substrate antenna materials is acceptable. Nonetheless, the reflection loss associated with the mismatch in the real antenna matching circuit is not accounted for. Mismatch and reflections can be fine-tuned throughout project execution in order to optimize a variety of performance trade-offs.

IV. ANTENNA MEASUREMENT

We fabricate and measure the antennas to validate the impedance bandwidth and radiation pattern of the proposed antenna through measurement using the R&S ZVA67 network analyzer. Figure 12 shows the fabrication results of the MF-PCF antenna using a Rogers 5880 substrate with a thickness of 1.57 mm. At the time of measurement, we use a 4-hole SMA female type port connector with a frequency

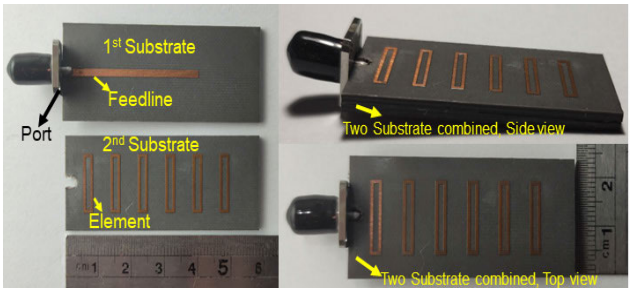

FIGURE 12. Microstrip antenna MF-PCF design obtained from the mathematical equations fabricated on Rogers 5880 materials.

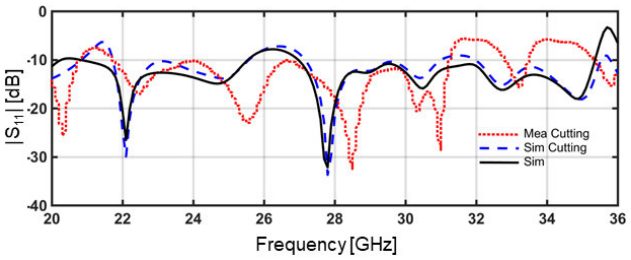

FIGURE 13. Return loss of six-element MF-PCF: simulation and fabrication.

of up to 40 GHz. From the measurement, it can be seen that the total length of the antenna is 58.32 mm, and the width is 24.12 mm, stacked between the first and second substrates.

A. IMPEDANCE BANDWIDTH

Figure 13 compares the return loss profiles of a six-element antenna obtained from the simulation and measurement results. We also carry out simulations by crossing the substrate at layer 2. The intersection is intended for placing ports on the feedline in the fabricated antenna. The reflection coefficient is shown in dotted blue line. The resulting incompatibilities are mainly due to fabrication imprecision and connector effects. Also, the mutual coupling associated with the gap between the patches, the feed line dimensions, and the folded stub gap is important for optimizing the return loss. See Table 5 for the comparison.

B. RADIATION PATTERN

Figure 14 shows similarities between simulation results and measurements. Namely, they both have three major lobes, each of which has a different direction. In the case of millimeter-wave frequency use, high gain is required to overcome path loss in LoS and NLoS environments.

In the process of measuring the radiation pattern, the placement of the transmitting and receiving antennas is such that the far field is achieved for the shortest wavelength, which can be calculated by

$$R \geq \frac{2D^2}{\lambda_{\min}} \tag{17}$$

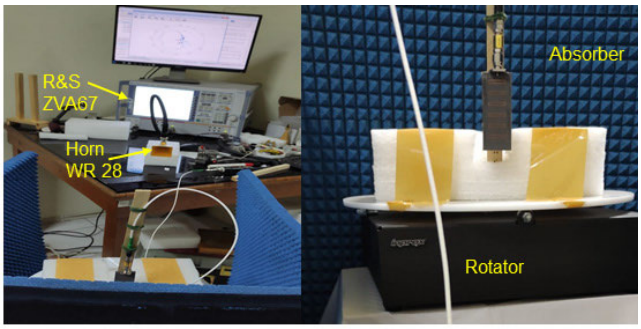

(a)

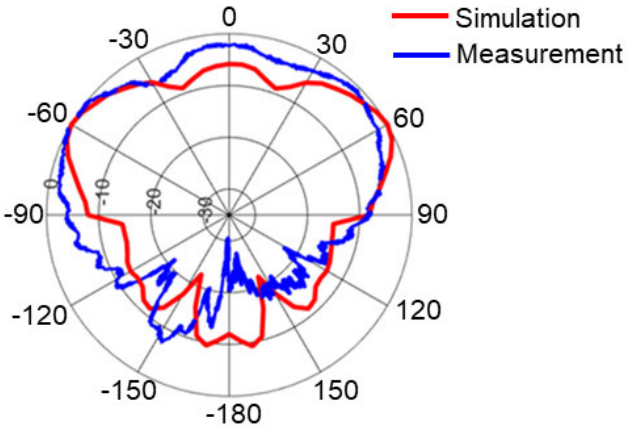

(b)

FIGURE 14. (a) Antenna measurement configuration setup (b) Simulated and measured normalized radiation patterns of the MF-PFC at 28 GHz.

TABLE 5. Simulation vs measurement results for 6-element MF-PCF.

Parameter	Simulation	Simulation Cutting Feed	Measurement Cutting Feed
Resonant frequency	22.1, 27.8 GHz	22.1, 27.8, 35 GHz	28.5, 33.2 GHz
Gain	11.55 dBi	11.84 dBi	-
Lowest return loss	-32.2 dB	-33.73 dB	-32.1 dB
Bandwidth	4.75 GHz (20.80-25.55 GHz)	3.85 GHz (21.72-25.57 GHz)	9.34 GHz (21.72-31.06 GHz)
	8.39 GHz (26.96–35.35 GHz)	3.86 GHz (27.15-31.01 GHz)	0.8 GHz (32.7-33.5 GHz)
		3.58 GHz (31.96-35.54 GHz)	

where R is the distance between the transmit antenna and the receive antenna (m), D the largest dimension of the antenna (m), and $\lambda_{\min}$ the shortest operating wavelength (m).

Table 6 compares the features between the proposed antenna and similar others. The comparison indicates that, among the antenna designs, the proposed MF-PCF antenna structure has several advantages, i.e., compact size, large

TABLE 6. Comparison of various antenna performance indicators.

Antenna Type	Center Frequency [GHz]	Bandwidth [GHz]	Gain [dBi]	Size [mm^2]
Dielectric slab antenna based on microstrip-Franklin excitation [7]	30	3.3	6.6	80×20
Franklin array antenna [39]	2.4	0.02	12	520×520
Franklin modification with line feeding and λ/2 stub [40]	24	0.25	10	90 × 25
Franklin with 6 patch elements [48]	29	5.4	8.3	28.2×12
Modified Franklin with 6 elements [54]	28	5.3	7.2	30×12.6
Franklin antenna with dual circular polarizations [55]	6.9	0.339	3.1	172×172
Proposed antenna	28	9.34	11.55	58×24

bandwidth, high gain, and simple structure, making it a strong contender for use in 5G technology.

V. CONCLUSION

This paper presents a Franklin microstrip design based on a series of equations drawn from many previous works into a single solution for a modified Franklin microstrip antenna using the proximity-coupled feedline (MF-PCF) technique. The application of both the Franklin technique and the PCF seeks to increase the bandwidth and gain impedance proportions with high precision. The proposed equivalent circuits and equations allow a simple but accurate model to be built for MF-PCF. The model is validated by measurement at millimeter-wave frequency. The resulting bandwidth and gain of the new MF-PCF design obtained from applying the equations are very similar to the simulation and measurement results. Specifically, from the simulation results, the largest bandwidth of 8.39 GHz is obtained with a frequency range of 26.96-35.35 GHz and gain of 11.55 dBi, while the largest bandwidth from measurement is 9.34 GHz with a frequency range of 21.96-31.06 GHz. Similarity in antenna radiation patterns is also observed from the simulations and measurements. Further comparison shows the advantages offered by the MF-PCF over other contending designs for 5G applications.

ACKNOWLEDGMENT

The authors are grateful to Mercu Buana University for providing simulation and measurement facilities used in this research.

REFERENCES

[1] *3rd Generation Partnership Project; Technical Specification Group Services and System Aspects Release 15 Description; Summary of Rel-15 Work Items*, document 3GPP TR 21.915, V 0.4.0, 3GPP, 2018. [Online]. Available: https://www.3gpp.org/

[2] *3rd Generation Partnership Project; Technical Specification Group Radio Access Network; User Equipment (UE) Radio Transmission and Reception (FDD)*, document 3GPP TS 25.101, v 6.12.0, 3GPP, 2019.

[3] *3rd Generation Partnership Project; Technical Specification Group Services and System Aspects; Service Requirements for the 5G System*, document 3GPP TS 22.261, 3GPP, 2020. [Online]. Available: https://www.3gpp.org/

[4] E. Obiodu. (2019). *The 5G Guide, A Reference for Operators*. [Online]. Available: https://www.gsmaintelligence.com

[5] R. Lionnie, L. Ruhyana, and M. Alaydrus, "Dual-band microstrip antennas for 5G and short-range applications," in *Proc. IEEE Region 10 Conf. (TENCON)*, Nov. 2017, pp. 2910–2913, doi: 10.1109/TENCON.2017.8228359.

[6] S. Mahon, "The 5G effect on RF filter technologies," *IEEE Trans. Semicond. Manuf.*, vol. 30, no. 4, pp. 494–499, Nov. 2017, doi: 10.1109/TSM.2017.2757879.

[7] E. C. V. Boas, A. A. C. Alves, J. A. J. Ribeiro, and A. S. Cerqueira, "A novel dielectric slab antenna based on microstrip-Franklin excitation for mm-waves," *J. Microw., Optoelectron. Electromagn. Appl.*, vol. 19, no. 2, pp. 203–213, Jun. 2020, doi: 10.1590/2179-10742020v19i2822.

[8] A. Firdausi, G. Hakim, and M. Alaydrus, "Designing a tri-band microstrip antenna for targetting 5G broadband communications," in *Proc. MATEC Web Conf.*, vol. 218, 2018, pp. 1–5, doi: 10.1051/matecconf/201821803015.

[9] M. Dogan, G. K. Sendur, and F. Ustuner, "Optimization of aperture coupled microstrip patch antennas," in *Proc. Prog. Electromagn. Res. Symp.*, 2010, pp. 657–660.

[10] J. Maharjan, S. W. Kim, and D.-Y. Choi, "Franklin array MIMO antenna for 5G applications," in *Proc. 34th Int. Tech. Conf. Circuits/Syst., Comput. Commun. (ITC-CSCC)*, Jun. 2019, pp. 1–4, doi: 10.1109/ITC-CSCC.2019.8793455.

[11] C. A. Balanis, *Antenna Theory: Analysis and Design*, 3rd ed. New York, NY, USA: Wiley, 2005.

[12] Z. Wang, J. Liu, and Y. Long, "A simple wide-bandwidth and high-gain microstrip patch antenna with both sides shorted," *IEEE Antennas Wireless Propag. Lett.*, vol. 18, no. 6, pp. 1144–1148, Jun. 2019, doi: 10.1109/LAWP.2019.2911045.

[13] A. Chen, Y. Zhang, Z. Chen, and S. Cao, "A *Ka*-band high-gain circularly polarized," *IEEE Antennas Wireless Propag. Lett.*, vol. 9, pp. 1115–1118, 2010.

[14] A. Firdausi, G. P. Nurani Hakim, and M. Alaydrus, "Microstrip antenna array for next generation WLAN 802.11ac applications," in *Proc. Int. Conf. Radar, Antenna, Microw., Electron., Telecommun. (ICRAMET)*, Nov. 2018, pp. 86–89, doi: 10.1109/ICRAMET.2018.8683939.

[15] K. D. Xu, H. Xu, Y. Liu, J. Li, and Q. H. Liu, "Microstrip patch antennas with multiple parasitic patches and shorting vias for bandwidth enhancement," *IEEE Access*, vol. 6, pp. 11624–11633, 2018, doi: 10.1109/ACCESS.2018.2794962.

[16] S.-H. Wi, Y.-S. Lee, and J.-G. Yook, "Wideband microstrip patch antenna with U-shaped parasitic elements," *IEEE Trans. Antennas Propag.*, vol. 55, no. 4, pp. 1196–1199, Apr. 2007, doi: 10.1109/TAP.2007.893427.

[17] S. T. Fan, Y. Z. Yin, B. Lee, W. Hu, and X. Yang, "Bandwidth enhancement of a printed slot antenna with a pair of parasitic patches," *IEEE Antennas Wireless Propag. Lett.*, vol. 11, pp. 1230–1233, 2012, doi: 10.1109/LAWP.2012.2224311.

[18] B. Yildirim and B. A. Cetiner, "Enhanced gain patch antenna with a rectangular loop shaped parasitic radiator," *IEEE Antennas Wireless Propag. Lett.*, vol. 7, pp. 229–232, 2008, doi: 10.1109/LAWP.2008.922313.

[19] Y. Cao, Y. Cai, W. Cao, B. Xi, Z. Qian, T. Wu, and L. Zhu, "Broadband and high-gain microstrip patch antenna loaded with parasitic mushroom-type structure," *IEEE Antennas Wireless Propag. Lett.*, vol. 18, no. 7, pp. 1405–1409, Jul. 2019, doi: 10.1109/LAWP.2019.2917909.

[20] A. Kumar and N. Gupta, "Gain and bandwidth enhancement techniques in microstrip patch Antennas–A review," *Int. J. Comput. Appl.*, vol. 148, no. 7, pp. 9–14, Aug. 2016, doi: 10.5120/ijca2016911207.

[21] M. M. Soliman, M. M. A. Faisal, Engr. M. J. Uddin, M. L. Hakim, M. Rahman, M. M. Billah, and M. N. C. Saddam, "Analytical review of bandwidth enhancement techniques of microstrip patch antenna," in *Proc. IEEE 5th Int. Conf. for Converg. Technol. (I2CT)*, Mar. 2019, pp. 1–5, doi: 10.1109/I2CT45611.2019.9033547.

[22] P. Kovacs, "High gain microstrip antenna using planar circularly symmetric EBG structures," in *Proc. 17th Int. Conf. Radioelektronika*, Brno, Czech Republic, 2007, pp. 1–5, doi: 10.1109/RADIOELEK.2007.371681.

[23] M. Kashani, L. Shafai, and D. Isleifson, "Performance improvement of a microstrip patch antenna on an EBG structure," in *Proc. IEEE Int. Symp. Antennas Propag. North Amer. Radio Sci. Meeting*, Montreal, QC, Canada, 2020, pp. 143–144, doi: 10.1109/IEEECONF35879.2020.9329903.
[24] Z.-J. Han, W. Song, and X.-Q. Sheng, "Gain enhancement and RCS reduction for patch antenna by using polarization-dependent EBG surface," *IEEE Antennas Wireless Propag. Lett.*, vol. 16, pp. 1631–1634, 2017, doi: 10.1109/LAWP.2017.2658195.
[25] S. M. Duffy, "An enhanced bandwidth design technique for electromagnetically coupled microstrip Antennas," *IEEE Trans. Antennas Propag.*, vol. 48, no. 2, pp. 161–164, Feb. 2000.
[26] K. Chattopadhyay, S. Mukherjee, S. Das, and S. R. B. Chaudhuri, "Bandwidth enhancement of microstrip dipole using proximity coupling method," in *Proc. IEEE Int. Symp. Antennas Propag. (APSURSI)*, Jul. 2011, pp. 1758–1761, doi: 10.1109/APS.2011.5996834.
[27] H. A. Diawuo and Y.-B. Jung, "Broadband proximity-coupled microstrip planar antenna array for 5G cellular applications," *IEEE Antennas Wireless Propag. Lett.*, vol. 17, no. 7, pp. 1286–1290, Jul. 2018, doi: 10.1109/LAWP.2018.2842242.
[28] H.-T. Hu, B.-J. Chen, and C. H. Chan, "A transparent proximity-coupled-fed patch antenna with enhanced bandwidth and filtering response," *IEEE Access*, vol. 9, pp. 32774–32780, 2021, doi: 10.1109/ACCESS.2021.3061203.
[29] S. Akinola, I. Hashimu, and G. Singh, "Gain and bandwidth enhancement techniques of microstrip antenna: A technical review," in *Proc. Int. Conf. Comput. Intell. Knowl. Economy (ICCIKE)*, Dec. 2019, pp. 175–180, doi: 10.1109/ICCIKE47802.2019.9004278.
[30] H. Tian, C. Liu, and X. Gu, "Proximity-coupled feed patch antenna array for 79 GHz automotive radar," *J. Eng.*, vol. 2019, no. 19, pp. 6244–6246, Oct. 2019, doi: 10.1049/joe.2019.0262.
[31] S. F. Maharimi, M. F. A. Malek, M. F. Jamlos, S. C. Neoh, and M. Jusoh, "Impact of spacing and number of elements on array factor," in *Proc. Prog. Electromagn. Res. Symp.*, vol. 2014, 2012, pp. 1550–1553.
[32] C. S. Franklin, "Improvements in wireless telegraph and telephone aerials," U.K. British Patent 242 342, Nov. 5, 1925.
[33] S. Nishimura, K. Nakano, and T. Makimoto, "Franklin type microstrip line antenna," in *Proc. Antennas Propag. Soc. Int. Symp.*, vol. 2, Jun. 1979, pp. 134–137, doi: 10.1109/APS.1979.1148179.
[34] E. Lee, K. M. Chan, P. Gardner, and T. E. Dodgson, "Active integrated antenna design using a contact-less, proximity coupled, differentially fed technique," *IEEE Trans. Antennas Propag.*, vol. 55, no. 2, pp. 267–276, Feb. 2007, doi: 10.1109/TAP.2006.889828.
[35] A. Holub and M. Polivk, "Collinear microstrip patch antennas," in *Passive Microwave Components and Antennas*. Rijeka, Croatia: InTech, Apr. 2010, doi: 10.5772/9396.
[36] M. Polivka, A. Holub, and M. Mazanek, "Collinear microstrip patch antenna," *Radioengineering*, vol. 14, no. 4, pp. 40–42, 2005, doi: 10.5772/9396.
[37] M. Polivka and A. Holub, "Planar version of collinear microstrip patch antenna," in *Proc. Int. Conf. Microw., Radar Wireless Commun.*, May 2006, pp. 7–10.
[38] P. P. Wang, M. A. Antoniades, and G. V. Eleftheriades, "An investigation of printed Franklin antennas at X-band using artificial (metamaterial) phase-shifting lines," *IEEE Trans. Antennas Propag.*, vol. 56, no. 10, pp. 3118–3128, Oct. 2008, doi: 10.1109/TAP.2008.929455.
[39] S. H. Chang, W. J. Liao, K. W. Peng, and C. Y. Hsieh, "A Franklin array antenna for wireless charging applications," in *Proc. Prog. Electromagn. Res. Symp.*, vol. 1, 2010, pp. 269–273, doi: 10.2529/piers090904050641.
[40] C.-H. Kuo, C.-C. Lin, and J.-S. Sun, "Modified microstrip Franklin array antenna for automotive short-range radar application in blind spot information system," *IEEE Antennas Wireless Propag. Lett.*, vol. 16, pp. 1731–1734, 2017, doi: 10.1109/LAWP.2017.2670231.
[41] S. F. Jilani and A. Alomainy, "A multiband millimeter-wave 2-D array based on enhanced Franklin antenna for 5G wireless systems," *IEEE Antennas Wireless Propag. Lett.*, vol. 16, pp. 2983–2986, 2017, doi: 10.1109/LAWP.2017.2756560.
[42] O. Niksan, M. Bemani, and A. Farzamnia, "A compact multi-band mm-wave Franklin array with frequency scanning capability," in *Proc. 6th Iranian Conf. Radar Surveill. Syst.*, Dec. 2019, pp. 1–6, doi: 10.1109/ICRSS48293.2019.9026556.
[43] S.-W. Qu and Q. Xue, "A Y-shaped stub proximity coupled V-slot microstrip patch antenna," *IEEE Antennas Wireless Propag. Lett.*, vol. 6, pp. 40–42, 2007, doi: 10.1109/LAWP.2007.891515.
[44] D. M. Pozar and B. Kaufman, "Increasing the bandwidth of a microstrip antenna by proximity coupling," *Electron. Lett.*, vol. 23, no. 8, pp. 368–369, Apr. 1987, doi: 10.1049/el:19870270.
[45] G. Kumar and K. P. Ray, *Broadband Microstrip Antennas*. Boston, MA, USA: Artech House, 2003.
[46] S. J. Orfanidis, *Electromagnetic Waves and Antennas*. New Brunswick, NJ, USA: Rutgers Univ., 2008.
[47] T. A. Milligan, *Modern Antenna Design*. Hoboken, NJ, USA: Wiley, 2005, doi: 10.1002/0471720615.
[48] S. F. Jilani and A. Alomainy, "Millimeter-wave conformal antenna array for 5G wireless applications," in *Proc. IEEE Int. Symp. Antennas Propag. USNC/URSI Nat. Radio Sci. Meeting*, Jul. 2017, pp. 1439–1440, doi: 10.1109/APUSNCURSINRSM.2017.8072762.
[49] R. Garg, P. Bhartia, I. Bahl, and A. Ittipiboon, *Microstrip Antenna Design Handbook*. Norwood, MA, USA: Artech House, 2001.
[50] N. Aboserwal, N. R. Ccoillo Ramos, Z. Qamar, and J. L. Salazar-Cerreno, "An accurate analytical model to calculate the impedance bandwidth of a proximity coupled microstrip patch antenna (PC-MSPA)," *IEEE Access*, vol. 8, pp. 41784–41793, 2020, doi: 10.1109/ACCESS.2020.2976750.
[51] A. A. Al-Behadili, I. A. Mocanu, N. Codreanu, and M. Pantazica, "Modified split ring resonators sensor for accurate complex permittivity measurements of solid dielectrics," *Sensors*, vol. 20, no. 23, p. 6855, Nov. 2020, doi: 10.3390/s20236855.
[52] A. Firdausi, G. Hendrantoro, E. Setijadi, and M. Alaydrus, "Dual mode on-body off-body microstrip antenna Franklin for wearable device over 5G application," in *Proc. IEEE Microw., Antennas, Propag. Conf. (MAPCON)*, Dec. 2022, pp. 1999–2004, doi: 10.1109/MAPCON56011.2022.10047627.
[53] D. Guha, "Resonant frequency of circular microstrip antennas with and without air gaps," *IEEE Trans. Antennas Propag.*, vol. 49, no. 1, pp. 55–59, Jan. 2001, doi: 10.1109/8.910530.
[54] S. F. Jilani, Q. H. Abbasi, Z. U. Khan, T. Loh, and A. Alomainy, "A Ka-band antenna based on an enhanced Franklin model for 5G cellular networks," *Microw. Opt. Technol. Lett.*, vol. 60, no. 6, pp. 1562–1566, Jun. 2018, doi: 10.1002/mop.31194.
[55] S. Chaudhuri, R. S. Kshetrimayum, and R. K. Sonkar, "High inter-port isolation dual circularly polarized slot antenna with interdigital capacitor," *Int. J. RF Microw. Comput.-Aided Eng.*, vol. 29, no. 10, pp. 2019–2022, Oct. 2019, doi: 10.1002/mmce.21903.

AHMAD FIRDAUSI (Student Member, IEEE) received the bachelor's and master's degrees in electrical engineering with specialization in antenna design. He is currently pursuing the Ph.D. degree in electrical engineering with Institut Teknologi Sepuluh Nopember (ITS), Surabaya, Indonesia. His research interests include radio-frequency (RF) circuit design, radio-frequency identification (RFID), signals and systems, wearable and flexible antennas, metamaterial-based antennas, implantable antennas, multi-input-multi-output (MIMO) antennas, mm-wave antennas, 5G antennas, antenna arrays, metasurfaces antennas, dielectric resonator antennas (DRAs), photonic antennas, antenna for the Internet of Things applications, ultra-wideband (UWB) antennas, wideband antennas, reconfigurable antennas, terahertz antennas, rectennas for energy harvesting applications, active sensors, and the IoT-based communication devices. He is a member of the IEEE Antennas and Propagation Society.

GAMANTYO HENDRANTORO (Senior Member, IEEE) was born in Jombang, Indonesia, in November 1970. He received the B.Eng. degree in electrical engineering from Institut Teknologi Sepuluh Nopember (ITS), Surabaya, Indonesia, in 1992, and the M.Eng. and Ph.D. degrees in electrical engineering from Carleton University, Ottawa, Canada, in 1997 and 2001, respectively. He is currently a Professor with the Department of Electrical Engineering, ITS. He has been involved in various projects, including investigation into millimeter-wave radio channel modeling and wireless systems for tropical regions, studies on HF skywave channels and communications in equatorial regions, and development of array and signal processing for MIMO radars. His current research interests include multi-beam OFDM MIMO radar and 5G/6G wireless channels and communication systems. He received the R. F. Chinnick Scholarship Award from Telesat Canada, the Post-Graduate Research Excellence Award from the Canadian Institute for Telecommunications Research (CITR), and the Young Scientist Award from the International Union of Radio Science (URSI). He is the 2023 Chair of the IEEE Indonesia Section.

EKO SETIJADI (Member, IEEE) was born in Indonesia, in October 1972. He received the B.Eng. and M.Eng. degrees in electrical engineering from Institut Teknologi Sepuluh Nopember (ITS), Surabaya, Indonesia, and the Ph.D. degree in electrical engineering from Kumamoto University, Japan. He is currently an Associate Professor with the Department of Electrical Engineering, ITS. His current research interests include antenna design, microwave circuits, and metamaterials, including metasurface for communication and radar applications, electromagnetic compatibility, communication network design and optimization, and engineering education.

MUDRIK ALAYDRUS (Senior Member, IEEE) received the Dr.-Ing. degree in electrical engineering with specialization in electromagnetics. From 1997 to 2002, he was a Researcher with the Chair of Electromagnetics, University of Wuppertal, Germany. Since 2003, he has been with Universitas Mercu Buana, Jakarta. He is currently a Professor with the Department of Electrical Engineering, Universitas Mercu Buana. He has more than 200 publications in journals and conferences, wrote four books in transmission lines, antennas, and electromagnetic fields and microwave engineering, all in Indonesian. He holds two patents. His research interests include electromagnetics, microwave and millimeter waves, as well as mathematical approaches for signal processing. He is a member of Verein Deutscher Elektroingenieure (VDE) as well as a member of Persatuan Insinyur Indonesia (PII). He was the Chair of the Joint AP/MTT Indonesia Chapter.